CHALMERS
UNIVERSITY OF TECHNOLOGY

Defects from phonons: Atomic transport by concerted motion in simple crystalline metals

Acta Materialia 196 (2020) 770–775

Contents lists available at ScienceDirect

Acta Materialia

journal homepage: www.elsevier.com/locate/actamat

Full length article

Defects from phonons: Atomic transport by concerted motion in simple crystalline metals

Erik Fransson, Paul Erhart*

Chalmers University of Technology, Department of Physics, Gothenburg S-412 96, Sweden

ARTICLE INFO

Article history:
Received 5 February 2020
Revised 4 May 2020
Accepted 17 June 2020
Available online 27 June 2020

ABSTRACT

Point defects play a crucial role in crystalline materials as they do not only impact the thermodynamic properties but are also central to kinetic processes. While they are necessary in thermodynamic equilibrium spontaneous defect formation in the bulk is normally considered highly improbable except for temperatures close to the melting point. Here, we demonstrate by means of atomistic simulations that processes involving concerted atomic motion that give rise to defect formation are in fact frequent in body-centered cubic metals even down to about 50% of the melting temperature. It is shown that this behavior is intimately related to the anharmonicity of the lattice vibrations and a flat energy landscape along certain crystallographic directions, a feature that is absent in, e.g., face-centered cubic lattice structures. This insight has implications for our general understanding of these materials and furthermore provides a complementary explanation for the so-called anomalous diffusion in group 4 transition metals.

1. Introduction

Real crystalline materials contain point defects, such as vacancies and interstitials, which have a crucial impact on material properties including, e.g., kinetics, phase equilibrium, electrical and thermal transport as well as optical properties. Unlike one or two-dimensional defects such as dislocations or stacking faults, these zero-dimensional defects are thermodynamically necessary. Especially in more densely packed crystal structures such as face-centered cubic (FCC) or body-centered cubic (BCC) lattices, the equilibrium concentration of point defects at a given temperature is commonly established by exchange with an external reservoir such as a surface. Defect formation can also be induced in the bulk by external means such as irradiation with ions or high energy photons [1,2]. By contrast, *spontaneous* defect formation in the bulk is usually considered only close to the melting point [3,4].

Theoretical studies of superheated crystals have revealed that collective atomic motion, driven by point defects, is critical for destabilizing the lattice and nucleate melting [3,5]. Studies of atomic dynamics in glasses and liquids have identified related processes where atoms move collectively in string-like fashion with neighboring atoms being unaffected [6]. In these systems this collective motion has been connected to the phonon dispersion as well as a pronounced boson peak [5,7,8]. Interestingly, phonons are also known to be related to self-diffusion in crystalline materials and, in particular, many studies have been carried out concerning the phonon driven diffusion in BCC metals [9–14]. Furthermore, in BCC Ti as well as in BCC Fe (under inner-core conditions) the phonon modes in question have been connected to diffusion via concerted motion of a collection of atoms [15,16]. Finally, we note that in FCC materials grain boundary rearrangement through coordinated shuffling of atoms has been observed well below the melting temperatures [17].

Here, we demonstrate that spontaneous defect formation occurs in BCC metals with high frequency down to about 50% of the melting temperature. Our analysis reveals that the nucleation of vacancy-interstitial (Frenkel) pairs is the result of concerted atomic motion along close-packed ⟨111⟩ directions, similar to the collective atomic motion in superheated crystals, glasses and liquids. We establish a clear connection between these processes and specific phonon modes that turn out to be the same phonon modes that have previously been analyzed in connection with diffusion [9–13,18]. This enables us to identify the key features of the potential energy surface (PES), which are responsible for the observed behavior, and reveal trends across groups of materials. We show that the same principles and behavior can be found in FCC metals. The insight obtained in this fashion not only has consequences for our general understanding of defects but suggests a

* Corresponding author.
E-mail address: erhart@chalmers.se (P. Erhart).

https://doi.org/10.1016/j.actamat.2020.06.040

complementary explanation for the non-Arrhenius-like self-diffusion in group 4 metals. Previous studies have suggested that the strong temperature dependence of phonon frequencies induces changes in defect migration barriers [9–11,19]. The present results, however, demonstrate that the defect concentration itself (and not just the migration rate) can strongly deviate from an exponential temperature dependence. This is in line with other computational studies that have shown that vacancy concentrations in metals can exhibit non-Arrhenius behavior as a result of a temperature dependent free energy of defect formation [20–22], albeit to a weaker extent than shown here.

After summarizing our computational approach, we first describe the variation of defect pair concentrations as a function of temperature for a range of metals. Then, we resolve the atomistic mechanisms that gives rise to spontaneous defect formation and establish a relation to phonon dispersion and PES. Finally, we discuss the implications of the results and the effect of PES and lattice structure.

2. Methodology

Extensive molecular dynamics (MD) simulations were carried out for a range of BCC (Ti, Zr, Ta, Nb, Mo, W) and FCC metals (Al, Cu, Ni) using the LAMMPS code [23]. Temperature and pressure were controlled using Nosé-Hoover thermostat and barostat. First, the equilibrium lattice constants as a function of temperature were determined from *NPT* simulations. Subsequently, defect concentrations were obtained from *NVT* simulations at the respective lattice constants, which were run for up to 100 ns with a timestep of 2 fs and for systems with up to 500,000 atoms. Such large system are required to achieve convergence of the defect concentrations (see Fig. S1 in the Supplementary Material and discussion below). Periodic boundary conditions were applied in all directions and the simulations were started from perfect (defect free) systems. All defects observed in the simulations were thus the result of spontaneous formation in the bulk. We sampled temperatures between 115 and 60% of the melting temperature T_m and conducted a careful convergence study of the results with respect to system size (see Fig. S1 in the Supplementary Material for an example). The atomic interactions were described using embedded atom method (Al: [24], Cu: [25], Ni: [26], Ta: [27], Nb: [28], Zr: [29], W: [30]) and modified embedded atom method (Ti: [31], Mo: [32]) potentials. We emphasize that these potentials have been carefully benchmarked, already during their construction, with respect to their description of defect properties using data from both experiment and first-principles calculations. Further details can be found in the original references. They also provide sound predictions for the melting points (see Table S1 in the Supplementary Material).

The simulation data were analyzed using the atomic simulation environment ASE [33] as well as the open visualization tool OVITO [34]. Defects were identified by analyzing the occupancies of the Wigner–Seitz cells of the respective ideal lattice [35]. The phonon dispersion in Fig. 3e was obtained by analyzing the current density correlation functions from MD simulations using the DYNASOR package [36].

3. Results and discussion

3.1. Defect concentrations

In our MD simulations, which start from an ideal defect-free state, we observe a finite concentration of defects. Due to the absence of surfaces, these defects are the result of the spontaneous nucleation of vacancy-interstitial (Frenkel) pairs. The concentrations of these defect pairs exhibit an exponential temperature dependence

$$c \propto \exp(-E_A/k_BT)$$

over the entire temperature range, with the exception of the group 4 elements Ti and Zr (Fig. 1). The latter two metals display a deviation from exponential behavior, which we attribute to the strong anharmonicity of these materials.

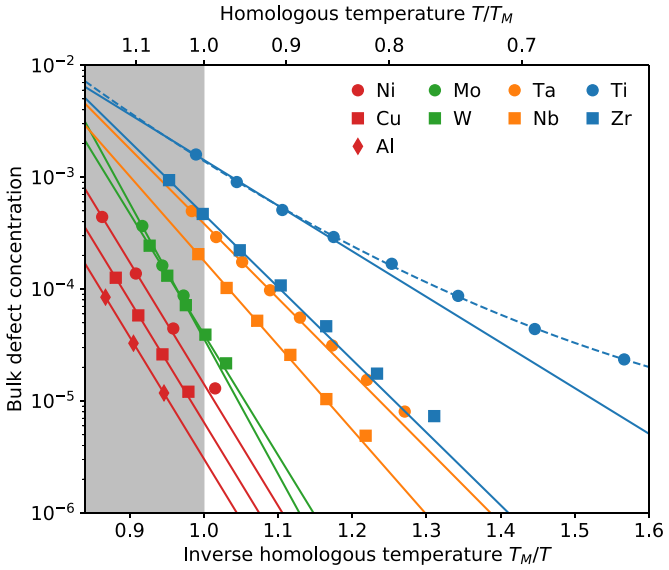

Fig. 1. Concentration of vacancy-interstitial pairs due to spontaneous defect formation in bulk BCC (Mo, W, Ta, Nb, Ti, Zr) and FCC (Ni, Cu, Al) metals from MD simulations. Solid lines represent fits to $c \propto \exp(-\beta E_A)$ where E_A is the activation energy for spontaneous defect formation (see Table S1). The dashed line is a higher order exponential fit to the Titanium concentrations, corresponding to $c \propto \exp(-\beta E_A^0 - (\beta E_C)^2)$ with $E_A^0 = 2.91$ eV and $E_C = -0.11$ eV. The gray shaded area marks the superheated region corresponding to temperatures above the melting point T_m. While in FCC metals defect concentrations are very small up to the melting point, in BCC metals defect concentration are several orders of magnitude larger and as a result are already substantial far below melting. Estimated 95% confidence interval errors for the data points are typically substantially smaller than the symbols used in this figure.

Defect concentrations are particularly high in group 3 (Ta, Nb) and 4 (Ti, Zr) metals, for which values above 10^{-5} (the lower detection limit in our simulations) are observed down to homologous temperatures T/T_m of 0.64 (Ti), 0.76-0.78 (Zr, Ta), and 0.82 (Nb). While for vacancies the resulting concentrations are smaller than the values obtained from the defect formation energies (Table S2 in the SI), the situation is reversed for interstitials. In the case of Ti and Zr, the BCC phase only appears at high temperatures and is stabilized by strongly anharmonic lattice vibrations. Yet high defect concentrations are also obtained for Ta and Nb, which have BCC ground state structures at low temperatures.

For the group 6 elements (Mo, W) and even more so the FCC elements (Al, Cu, Ni), defect concentrations are generally much smaller. This is particularly evident at the melting point, at which the concentration of spontaneously formed Frenkel pairs varies from 10^{-3} for Ti to 3×10^{-6} for Al, the latter value being extrapolated from higher temperatures. The presence of these defects is actually crucial for the melting process itself, in which defects are known to play an important role [3]. In the case of the group 6 BCC and FCC elements, the relatively low defect concentrations actually enable us to superheat (on the timescale of the present simulations) the crystalline phase far into the stability range of the liquid phase.

Generally, we observe that for defect concentrations $\gtrsim 10^{-3}$ nucleation of the liquid phase is all but inevitable. In the case of Ti, this limit is already reached at $T/T_m \approx 1$, whereas for Al a value of

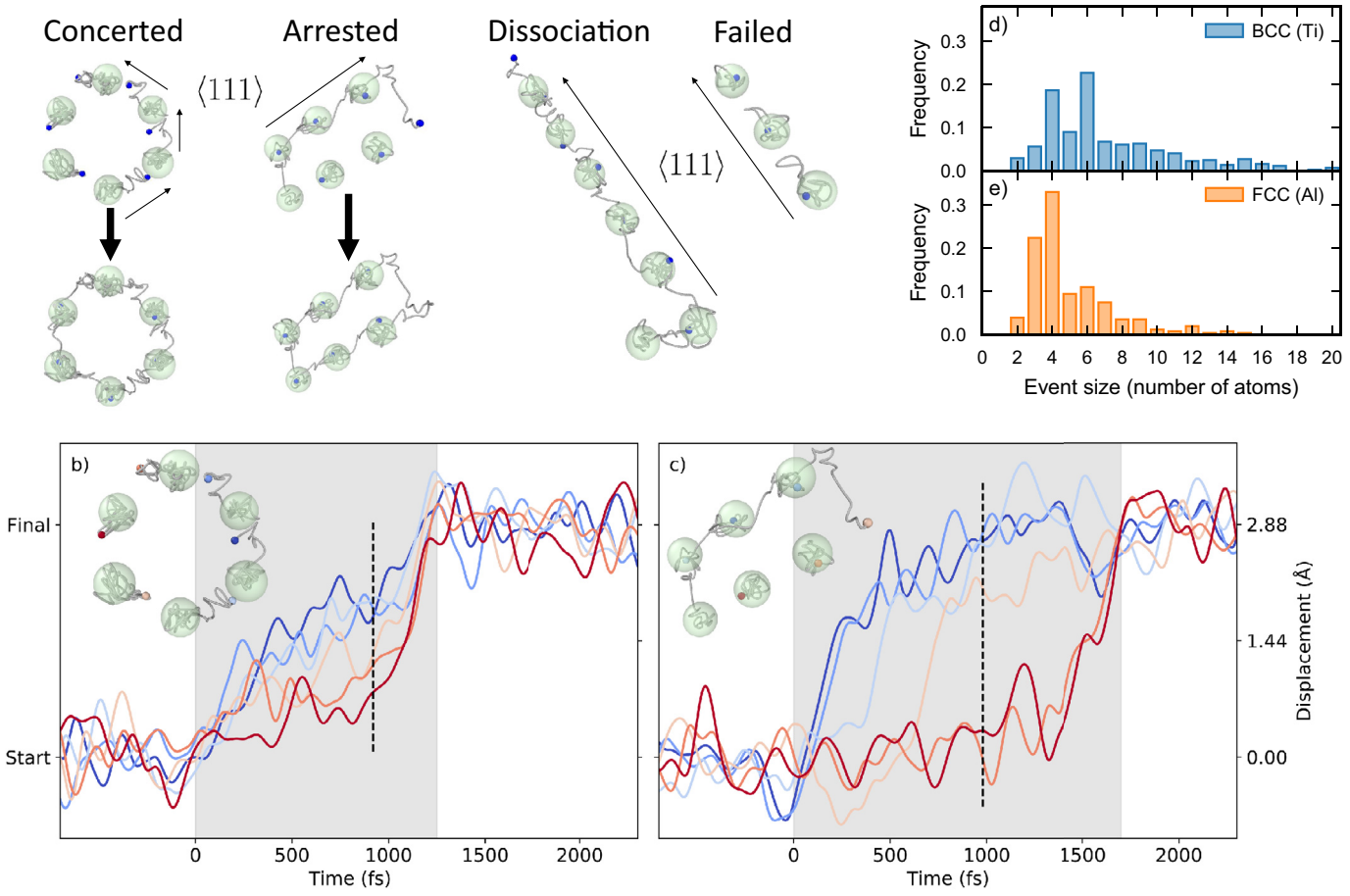

Fig. 2. (a) Atomic scale events related to the formation of vacancy-interstitial pairs in BCC metals. Small blue spheres mark atomic positions, green transparent spheres mark the initial atomic sites with the size indicating typical thermal displacements, and the gray lines indicate the atomic trajectories since the beginning of the event. Atomic displacements during (b) a concerted (ring-like) exchange event leading to atom exchange but no defect formation and (c) an arrested exchange event leading to the intermediate formation of an interstitial and a vacancy. Note that all atomic displacements occur between nearest neighbor sites and hence along ⟨111⟩ directions. Movies of the events are provided in the Supplementary Material. Frequency of events by size for (d) Ti and (e) Al. (For interpretation of the references to colour in this figure legend, the reader is referred to the web version of this article.)

$T/T_m \approx 1.35$ can be estimated by extrapolation of the available data. The activation energies E_A normalized by the melting temperature, $\alpha = E_A/k_B T_m$, exhibit similar group specific trends. While α ranges from 9.4 (Ti) to 17.4 (Nb) for groups 4 (Ti, Zr) and 5 (Ta, Nb), the values for group 6 (Mo, W) as well as the FCC metals (Al, Cu, Ni) are about 25 and larger indicating a much steeper temperature dependence.

3.2. Defect formation mechanisms

The systematic observation of spontaneous defect formation naturally leads to the question which fundamental principles govern this behavior. Firstly, it is instructive to explore the formation mechanism in detail. To this end, we analyzed up to 500 trajectories for three BCC (Ti, Ta, W) and one FCC metal (Al) with a time resolution of 10 fs, which allowed us to gather statistics at temperatures corresponding to a defect concentration of roughly 1.5×10^{-4}. In the following, we focus on the results for Ti and Al; results for other materials can be found in the Supplementary Material (Fig. S2).

Both BCC and FCC metals exhibit ring-like exchange mechanisms involving up to approximately six atoms, after which all atoms occupy regular lattice sites again (Fig. 2a,b) and Movie 1 in the Supplementary Material][1]. These events, however, do not lead to defect formation. Alternatively, the concerted motion of a string of atoms can become arrested and even break up into substrings (Fig. 2a,c and Movie 2 in the Supplementary Material], at which point the leading part of the string becomes an interstitial whereas the trailing part leaves behind a vacancy. Subsequently, the two defects thus formed migrate independently before either recombining with each other or other defects in the system. In the case of small ring-like exchange events, *all* atoms move at the same time (Fig. 2b). By contrast in the larger events, several *but not all* atoms move synchronously leading to the formation of an interstitial and a vacancy that are relatively close to each other, which can subsequently either recombine with each other by a sequence of individual defect migration events (arrested event in Fig. 2a) or migrate away from each other and thus become truly independent defects (dissociation event in Fig. 2a). During their respective lifetimes these individual defects contribute to the thermodynamic equilibrium concentration of vacancies and interstitials. Their lifetimes are determined by the time it takes to recombine with another opposing defect and are thus dependent on the overall defect concentration. This causes the concentration of spontaneously

[1] We note that isolated events similar to the ones described here have also been observed in ab-initio MD simulations of BCC-Ti close to the melting point, albeit for very small cells (54 atoms) and much shorter time scales, Ref. [37].

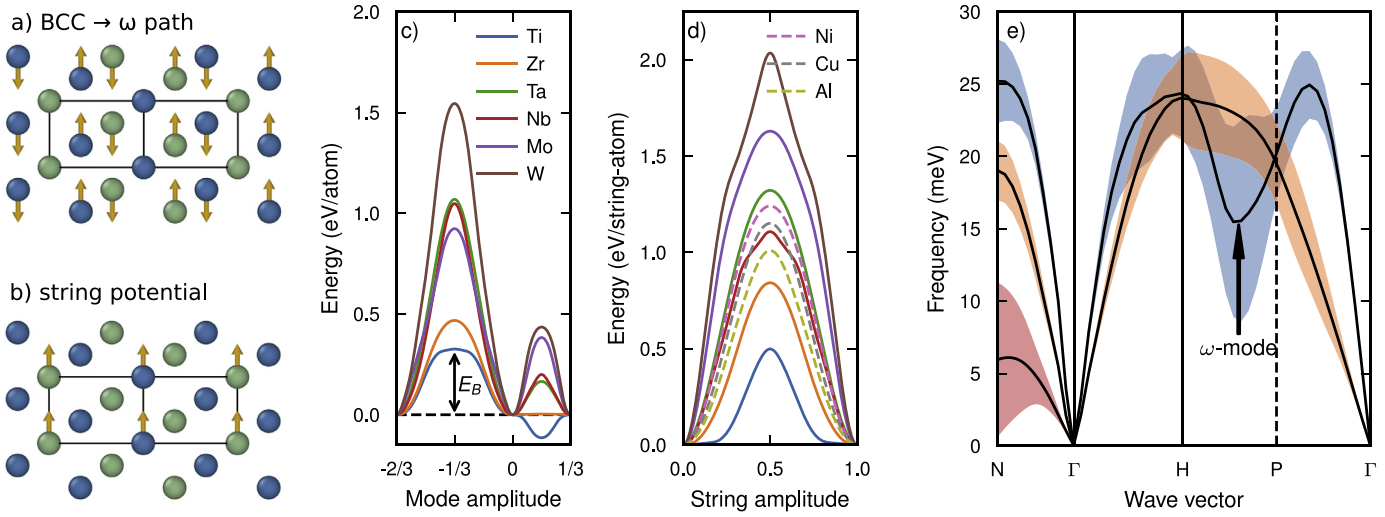

Fig. 3. (a) Atomic displacement pattern and (c) PESs associated with the longitudinal acoustic mode at $\vec{q} = \frac{2}{3}[1,1,1]$ corresponding to a transition path between the BCC and ω structures. (b) Atomic displacement pattern and (d) PESs associated with the string potential. The latter panel includes data not only for BCC but also FCC structures. The mode amplitude in (b) and the string amplitude in (d) are given in units of one repetitive unit. The mode and string amplitudes are normalized to the periodicity of the lattice. In (d) this corresponds to a displacement of the string of $\sqrt{3}/2a_0$ for BCC and $a_0/\sqrt{2}$ for FCC metals. (e) Phonon dispersion relation for BCC Ti at 1400 K computed from MD simulations. The shaded regions indicate the phonon lifetimes.

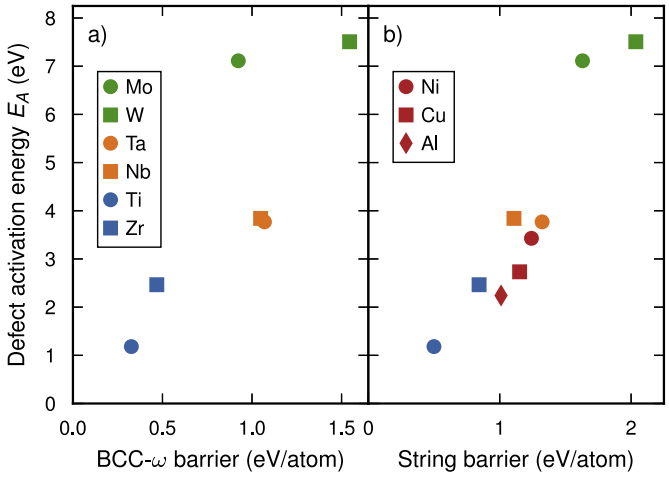

Fig. 4. Correlation of the defect activation energy with (a) the barrier between two BCC structures along the BCC → ω mode (Fig. 3c) and (b) the string potential barrier (Fig. 3d).

formed defects to have a strong system size dependence and requires very large simulation cells to achieve convergence at low temperatures (see Fig. S1 in the Supplementary Material).

The FCC lattice structure has a higher packing density than the BCC structure, which leads to the question whether defect formation via spontaneous atom exchanged is generally more prevalent in more open structures. We therefore also conducted MD simulations for silicon, for which a concerted exchange event has already been proposed as a means of diffusion [38]. In this case we found that 99% of the observed events involved only two atoms and did *not* lead to the formation of individual defects. In the more open diamond structure two atoms can thus exchange their positions with a rather limited impact on the surrounding atoms and the probability to observe larger (string-like) events is much lower than in more densely packed structures. This suggests that intermediate (BCC) to high (FCC) packing densities are crucial to obtain a larger number of events that involve several atoms. Larger events in turn are a prerequisite to separate atoms spatially preventing immediate recombination and thus enabling the formation of independent defects.

According to a detailed analysis of the nucleation and migration events, the nucleation as well as migration of a defect pair in BCC is predominantly the result of concerted atomic motion along close packed ⟨111⟩ directions. The shortest closed strings of atoms that can be constructed by concatenation of these directions involve either four or six atoms, which explains the predominance of events of these sizes in the event distribution for BCC metals (Fig. 2d). Similarly, in FCC systems we find defect nucleation to involve strings of atoms moving along close-packed ⟨110⟩ directions. The geometry of the lattice then allows for four-membered rings whereas one cannot construct equally compact six-membered rings. Accordingly, in the event size distribution there is a pronounced peak at four. For both BCC and FCC metals the distribution exhibits a heavy tail, which is the result of larger dissociation events (Fig. 2a).

3.3. Relation to phonon dispersion and defect migration

The preferential motion along close-packed directions is familiar from the migration of self-interstitial atoms [39]. The latter exhibit crowdion characteristics in the BCC metals considered here and their energetics can be well described using Frenkel-Kontorova models [30,40]. These models require as material specific input the so-called string or interrow potential, which describes the PES as a function of the displacement of a string of atoms along ⟨111⟩ (Fig. 3a,c). Our calculations show that the maxima of the string potential for a set of materials correlate with the defect concentrations as well as the defect activation energies (Fig. 4), where the latter can be extracted from the concentration vs temperature data by fitting an exponential expression (solid lines in Fig. 1).

The parallel motion of ⟨111⟩ strings also plays a role in the transition from the BCC to the ω structure, which has been investigated in detail in the case of the group 4 elements [41–45]. The most compact path between these structures is related to the longitudinal acoustic mode at $\vec{q} = \frac{2}{3}[1,1,1]$. It can be represented using a 3-atom unit cell and from here on will be referred to as the

BCC $\rightarrow \omega$ mode (Fig. 3b). Unlike the string potential the BCC $\rightarrow \omega$ mode can be accessed experimentally and has been extensively characterized in the past [41–43]. The connection between the BCC $\rightarrow \omega$ mode and defect formation is particularly apparent in the case of BCC Ti, for which the phonon mode in question appears as a pronounced minimum along the H–P direction (Fig. 3e). Following the normal coordinate of this mode reveals a strongly anharmonic PES with a very small barrier of 0.32 eV/atom separating periodic images of the structure (Fig. 3d). Note that in these calculations we considered very large displacements beyond the range usually considered in phonon calculations, which reveal the periodic nature of the PES.

To explore the connection between the BCC $\rightarrow \omega$ mode and the concentration of defect pairs nucleated in the bulk further, we computed the PES also for the other BCC metals considered in this study (Fig. 3d). The maximum energy encountered along the BCC $\rightarrow \omega$ path $E_{\max}^{\mathrm{BCC}\rightarrow\omega}$ does indeed correlate strongly with the activation energy E_A observed for the concentration of defect pairs nucleated in the bulk (Fig. 4b). In the case of the group 4 metals (Ti, Zr) the PES also features a pronounced negative region indicating the mechanical instability of the BCC structure, which at the same time is responsible for its vibrational stabilization at high temperatures.

4. Conclusion

In conclusion, in this work we have demonstrated an unusually strong propensity of the BCC structure for intrinsic defect formation compared to other crystal structures. The concentration of point defects created *spontaneously in the bulk* can be as large as 10^{-3} at the melting point and be substantial ($> 10^{-5}$) down to approximately 50% of the melting point (Fig. 1). Spontaneous defect formation proceeds via the concerted (string-like) motion of atoms, which is most likely to occur along close-packed directions (Fig. 2). In order for an initial vacancy-interstitial pair to dissociate one requires at least four to six atoms to be involved in the process, a condition that is satisfied in more densely packed crystal structures such as BCC and FCC (as opposed to e.g., diamond). At the same time the barrier for atomic displacement along the close-packed direction should be sufficiently small. As a result of this interplay, spontaneous defect formation has been found to be particular prevalent in materials that adopt the BCC crystal structure. The displacement of strings of atoms in the BCC structure can be linked to the BCC $\rightarrow \omega$ phonon mode (Fig. 3) and one observes in fact a strong correlation between the defect formation activation energy and both string potential and BCC $\rightarrow \omega$ barrier (Fig. 4). This allows one to estimate the contribution of spontaneous defect formation from microscopic quantities that can be readily obtained also from first-principles calculations.

Declaration of Competing Interest

The authors declare that they have no known competing financial interests or personal relationships that could have appeared to influence the work reported in this paper.

Acknowledgments

This work was funded by the Knut and Alice Wallenberg Foundation (2014.0226) and the Swedish Research Council (2015-04153). Computer time allocations by the Swedish National Infrastructure for Computing at NSC (Linköping) and C3SE (Gothenburg) are gratefully acknowledged.

Supplementary material

Supplementary material associated with this article can be found, in the online version, at doi:10.1016/j.actamat.2020.06.040.

References

[1] R.S. Averback, T. Diaz de la Rubia, Displacement damage in irradiated metals and semiconductors, Solid State Physics 51 (1998) 281.
[2] S.L. Dudarev, Thermal mobility of interstitial defects in irradiated materials, Physical Review B 65 (2002) 224105, doi:10.1103/PhysRevB.65.224105.
[3] A. Samanta, M.E. Tuckerman, T.-Q. Yu, W. E, Microscopic mechanisms of equilibrium melting of a solid, Science 346 (6210) (2014) 729–732, doi:10.1126/science.1253810.
[4] N.V. Doan, Y. Adda, Nouveau mécanisme de diffusion dans les solides à haute température, Philos. Mag. A 56 (2) (1987) 269–283, doi:10.1080/01418618708205166.
[5] H. Zhang, M. Khalkhali, Q. Liu, J.F. Douglas, String-like cooperative motion in homogeneous melting, J. Chem. Phys. 138 (12) (2013) 12A538, doi:10.1063/1.4769267.
[6] K. Nordlund, Y. Ashkenazy, R.S. Averback, A.V. Granato, Strings and interstitials in liquids, glasses and crystals, Europhys. Lett. 71 (4) (2005) 625, doi:10.1209/epl/i2005-10132-1.
[7] A.I. Chumakov, I. Sergueev, U. van Bürck, W. Schirmacher, T. Asthalter, R. Rüffer, O. Leupold, W. Petry, Collective nature of the boson peak and universal transboson dynamics of glasses, Phys. Rev. Lett. 92 (2004) 245508, doi:10.1103/PhysRevLett.92.245508.
[8] H. Shintani, H. Tanaka, Universal link between the boson peak and transverse phonons in glass, Nat. Mater. 7 (2008) 870, doi:10.1038/nmat2293.
[9] C. Herzig, Soft phonons and diffusion systematics in BCC transition metals and alloys, Defect and Diffusion Forum (1993). doi: 10.4028/ www.scientific.net/DDF.95-98.203
[10] C. Herzig, U. Köhler, Anomalous self-diffusion in BCC IVB metals and alloys, Mater. Sci. Forum (1987). doi: 10.4028/ www.scientific.net/MSF.15-18.301
[11] U. Köhler, C. Herzig, On the anomalous self-diffusion in bcc. titanium, physica status solidi (b) 144 (1) (1987) 243–251, doi:10.1002/pssb.2221440122.
[12] C. Herzig, U. Köhler, The influence of scandium on the anomalous self-diffusion in b.c.c.-zirconium, Acta Metall. 35 (7) (1987) 1831–1837, doi:10.1016/0001-6160(87)90129-5.
[13] G. Vogl, W. Petry, T. Flottmann, A. Heiming, Direct determination of the self-diffusion mechanism in bcc β-titanium, Physical Review B 39 (8) (1989) 5025–5034, doi:10.1103/PhysRevB.39.5025.
[14] C. Herzig, U. Köhler, S.V. Divinski, Tracer diffusion and mechanism of non-arrhenius diffusion behavior of zr and nb in body-centered cubic zr–nb alloys, J. Appl. Phys. 85 (12) (1999) 8119–8130, doi:10.1063/1.370650.
[15] D.G. Sangiovanni, J. Klarbring, D. Smirnova, N.V. Skripnyak, D. Gambino, M. Mrovec, S.I. Simak, I.A. Abrikosov, Superioniclike diffusion in an elemental crystal: bcc titanium, Phys. Rev. Lett. 123 (10) (2019) 105501, doi:10.1103/PhysRevLett.123.105501.
[16] A.B. Belonoshko, T. Lukinov, J. Fu, J. Zhao, S. Davis, S.I. Simak, Stabilization of body-centred cubic iron under inner-core conditions, Nat. Geosci. 10 (4) (2017) 312–316, doi:10.1038/ngeo2892.
[17] C.P. Race, R. Hadian, J. von Pezold, B. Grabowski, J. Neugebauer, Mechanisms and kinetics of the migration of grain boundaries containing extended defects, Physical Review B 92 (17) (2015) 174115, doi:10.1103/PhysRevB.92.174115.
[18] W. Petry, T. Flottmann, A. Heiming, J. Trampenau, M. Alba, G. Vogl, Atomistic study of anomalous self-diffusion in bcc β-titanium, Phys. Rev. Lett. 61 (6) (1988) 722–725, doi:10.1103/PhysRevLett.61.722.
[19] A.G. Mikhin, Y.N. Osetsky, On normal and anomalous self-diffusion in body-centred cubic metals: a computer simulation study, J. Phys.: Condens. Matter 5 (49) (1993) 9121, doi:10.1088/0953-8984/5/49/014.
[20] A. Glensk, B. Grabowski, T. Hickel, J. Neugebauer, Breakdown of the arrhenius law in describing vacancy formation energies: the importance of local anharmonicity revealed by ab initio thermodynamics, Phys. Rev. X 4 (1) (2014) 011018, doi:10.1103/PhysRevX.4.011018.
[21] A.S. Bochkarev, A. van Roekeghem, S. Mossa, N. Mingo, Anharmonic thermodynamics of vacancies using a neural network potential, Physical Review Materials 3 (9) (2019) 093803, doi:10.1103/PhysRevMaterials.3.093803.
[22] D. Smirnova, S. Starikov, G.D. Leines, Y. Liang, N. Wang, M.N. Popov, I.A. Abrikosov, D.G. Sangiovanni, R. Drautz, M. Mrovec, Atomistic description of self-diffusion in molybdenum: a comparative theoretical study of non-arrhenius behavior, Physical Review Materials 4 (1) (2020) 013605, doi:10.1103/PhysRevMaterials.4.013605.
[23] S. Plimpton, Fast parallel algorithms for short-range molecular dynamics, J. Comput. Phys. 117 (1) (1995) 1, doi:10.1006/jcph.1995.1039.
[24] Y. Mishin, D. Farkas, M.J. Mehl, D.A. Papaconstantopoulos, Interatomic potentials for monoatomic metals from experimental data and *ab initio* calculations, Physical Review B 59 (5) (1999) 3393–3407, doi:10.1103/PhysRevB.59.3393.
[25] Y. Mishin, M.J. Mehl, D.A. Papaconstantopoulos, A.F. Voter, J.D. Kress, Structural stability and lattice defects in copper: ab initio, tight-binding, and embedded-atom calculations, Physical Review B 63 (22) (2001) 224106, doi:10.1103/PhysRevB.63.224106.

[26] M.I. Mendelev, M.J. Kramer, S.G. Hao, K.M. Ho, C.Z. Wang, Development of interatomic potentials appropriate for simulation of liquid and glass properties of $nizr_2$ alloy, Philos. Mag. 92 (35) (2012) 4454–4469, doi:10.1080/14786435.2012.712220.
[27] R. Ravelo, T.C. Germann, O. Guerrero, Q. An, B.L. Holian, Shock-induced plasticity in tantalum single crystals: interatomic potentials and large-scale molecular-dynamics simulations, Physical Review B 88 (13) (2013) 134101, doi:10.1103/PhysRevB.88.134101.
[28] M.R. Fellinger, H. Park, J.W. Wilkins, Force-matched embedded-atom method potential for niobium, Physical Review B 81 (14) (2010) 144119, doi:10.1103/PhysRevB.81.144119.
[29] M.I. Mendelev, G.J. Ackland, Development of an interatomic potential for the simulation of phase transformations in zirconium, Philos. Mag. Lett. 87 (5) (2007) 349–359, doi:10.1080/09500830701191393.
[30] P.M. Derlet, D. Nguyen-Manh, S.L. Dudarev, Multiscale modeling of crowdion and vacancy defects in body-centered-cubic transition metals, Physical Review B 76 (5) (2007) 054107, doi:10.1103/PhysRevB.76.054107.
[31] R.G. Hennig, T.J. Lenosky, D.R. Trinkle, S.P. Rudin, J.W. Wilkins, Classical potential describes martensitic phase transformations between the α, β, and ω titanium phases, Physical Review B 78 (5) (2008) 054121, doi:10.1103/PhysRevB.78.054121.
[32] H. Park, M.R. Fellinger, T.J. Lenosky, W.W. Tipton, D.R. Trinkle, S.P. Rudin, C. Woodward, J.W. Wilkins, R.G. Hennig, Ab initio based empirical potential used to study the mechanical properties of molybdenum, Physical Review B 85 (21) (2012) 214121, doi:10.1103/PhysRevB.85.214121.
[33] A.H. Larsen, J.J. Mortensen, J. Blomqvist, I.E. Castelli, R. Christensen, M. Dulak, J. Friis, M.N. Groves, B. Hammer, C. Hargus, E.D. Hermes, P.C. Jennings, P.B. Jensen, J. Kermode, J.R. Kitchin, E.L. Kolsbjerg, J. Kubal, Kristen Kaasbjerg, S. Lysgaard, J.B. Maronsson, T. Maxson, T. Olsen, L. Pastewka, Andrew Peterson, C. Rostgaard, J. Schiotz, O. Schütt, M. Strange, K.S. Thygesen, Tejs Vegge, L. Vilhelmsen, M. Walter, Z. Zeng, K.W. Jacobsen, The atomic simulation environment – a python library for working with atoms, J. Phys.: Condens. Matter 29 (27) (2017) 273002, doi:10.1088/1361-648X/aa680e.
[34] A. Stukowski, Visualization and analysis of atomistic simulation data with ovito–the open visualization tool, Modell. Simul. Mater. Sci. Eng. 18 (1) (2010) 015012, doi:10.1088/0965-0393/18/1/015012.
[35] P. Erhart, J. Marian, Calculation of the substitutional fraction of ion-implanted He in an α-Fe target, J. Nucl. Mater. 414 (2011) 426, doi:10.1016/j.jnucmat.2011.05.017.
[36] https://dynasor.materialsmodeling.org/.
[37] S. Kadkhodaei, Q.-J. Hong, A. van de Walle, Free energy calculation of mechanically unstable but dynamically stabilized bcc titanium, Physical Review B 95 (2017) 064101, doi:10.1103/PhysRevB.95.064101.
[38] K.C. Pandey, Diffusion without vacancies or interstitials: a new concerted exchange mechanism, Phys. Rev. Lett. 57 (18) (1986) 2287–2290, doi:10.1103/PhysRevLett.57.2287.
[39] D. Nguyen-Manh, A.P. Horsfield, S.L. Dudarev, Self-interstitial atom defects in bcc transition metals: group-specific trends, Physical Review B 73 (2) (2006) 020101, doi:10.1103/PhysRevB.73.020101.
[40] S.P. Fitzgerald, D. Nguyen-Manh, Peierls potential for crowdions in the bcc transition metals, Phys. Rev. Lett. 101 (2008) 115504, doi:10.1103/PhysRevLett.101.115504.
[41] J. Trampenau, A. Heiming, W. Petry, M. Alba, C. Herzig, W. Miekeley, H.R. Schober, Phonon dispersion of the bcc phase of group-IV metals. III. bcc hafnium, Physical Review B 43 (13) (1991) 10963–10969, doi:10.1103/PhysRevB.43.10963.
[42] W. Petry, A. Heiming, J. Trampenau, M. Alba, C. Herzig, H.R. Schober, G. Vogl, Phonon dispersion of the bcc phase of group-IV metals. i. bcc titanium, Physical Review B 43 (13) (1991) 10933–10947, doi:10.1103/PhysRevB.43.10933.
[43] A. Heiming, W. Petry, J. Trampenau, M. Alba, C. Herzig, H.R. Schober, G. Vogl, Phonon dispersion of the bcc phase of group-iv metals. ii. bcc zirconium, a model case of dynamical precursors of martensitic transitions, Physical Review B 43 (1991) 10948–10962, doi:10.1103/PhysRevB.43.10948.
[44] D.R. Trinkle, R.G. Hennig, S.G. Srinivasan, D.M. Hatch, M.D. Jones, H.T. Stokes, R.C. Albers, J.W. Wilkins, New mechanism for the α to ω martensitic transformation in pure titanium, Phys. Rev. Lett. 91 (02) (2003) 025701, doi:10.1103/PhysRevLett.91.025701.
[45] D. Korbmacher, A. Glensk, A.I. Duff, M.W. Finnis, B. Grabowski, J. Neugebauer, Ab initio based method to study structural phase transitions in dynamically unstable crystals, with new insights on the β to ω transformation in titanium, Physical Review B 100 (2019) 104110, doi:10.1103/PhysRevB.100.104110.